Antitumor Potential of Crown Ethers: Structure−Activity Relationships, Cell Cycle Disturbances, and Cell Death Studies of a Series of Ionophores

Marko Marjanović,[†] Marijeta Kralj,*[,†] Fran Supek,[‡] Leo Frkanec,[§] Ivo Piantanida,[§] Tomislav Šmuc,[‡] and Ljerka Tušek-Božić[||]

Laboratory of Functional Genomics, Division of Molecular Medicine, Laboratory for Information Systems, Division of Electronics, Laboratory of Supramolecular and Nucleoside Chemistry, Division of Organic Chemistry and Biochemistry, Laboratory for Chemical Kinetics and Atmospheric Chemistry, Division of Physical Chemistry, Rudjer Bošković Institute, Bijenička cesta 54, P.O. Box 180, HR-10002 Zagreb, Croatia

Received October 6, 2006

The present paper demonstrates the antiproliferative ability and structure−activity relationships (SAR) of 14 crown and aza-crown ether analogues on five tumor-cell types. The most active compounds were di-*tert*-butyldicyclohexano-18-crown-6 (**3**), which exhibited cytotoxicity in the submicromolar range, and di-*tert*-butyldibenzo-18-crown-6 (**5**) (IC_{50} values of ∼2 μM). Also, **3** and **5** induced marked influence on the cell cycle phase distribution—strong G1 arrest, followed by the induction of apoptosis. A computational SAR modeling effort offers insight into possible mechanisms of crown ether biological activity, presumably involving penetration into cell membranes, and points out structural features of molecules important for this activity. The results reveal that crown ethers possess marked tumor-cell growth inhibitory activity, the extent of which depends on the characteristics of the hydrophilic macrocylic cavity and the surrounding hydrophobic ring. Our work supports the hypothesis that crown ether compounds inhibit tumor-cell growth by disrupting potassium ion homeostasis, which in turn leads to cell cycle perturbations and apoptosis.

Introduction

Crown ethers are macrocyclic polyethers that are characterized by having a different number of ethylene oxide units, either substituted or unsubstituted, joined covalently in a macrocyclic ring so that in their simplest form they are cyclic oligomers of dioxane.[1] The central feature of these compounds, which have been extensively studied since their discovery nearly four decades ago,[2] is their ability to form stable and selective complexes with various inorganic and organic cations. Crown ethers and related compounds became a central part of development in supramolecular (host/guest) chemistry, and they are still a topic of great current interest.[3−5] Many different modifications of the crown ethers, such as changing the ring size, the kinds of substituents, and the types of donor atoms, have been made to enhance their complexation properties. The aza-crowns have complexation properties that are intermediate between those of all-oxygen crown ligands, which complex strongly with alkali, alkaline earth, and primary ammonium cations, and those of all-nitrogen cyclams, which complex strongly with the heavy metal cations.[6] Structurally, crown ethers possess a hydrophobic ring surrounding a hydrophilic cavity, which enables them to form stable complexes with metal ions, and at the same time to be incorporated in the lipid fraction of the cell membrane. Consequently, they exhibit ionophoretic properties in membranes, behaving very similarly to the natural ionophores, such as gramicidin, valinomycin, and so forth.[7,8] These characteristics make crown ethers particularly interesting and useful in chemical and biological research. For example, crown ethers have wide application as ion-chelating resins,[8] as sensors for a broad range of inorganic ions, and also have several applications in biology, such as regulating enzyme activity in the catalysis of reactions that use enzymes in organic solvents.[1] Furthermore, similarly to natural ionophores, crown ether compounds are also found to be toxic in prokaryotic and eukaryotic cellular systems,[1,9] which led to further studies on their potential for being developed as antimicrobial agents. Moreover, functionalized crowns have also been synthesized to bind and cleave DNA and have led to investigative drug studies in cancer research.[1] However, although some crown ether complexes with, for example, naphthoquinonethiol,[10] cisplatin derivatives,[11] or a bis-(propargilic) sulfone moiety,[12] showed good antitumor and/or antimicrobial activities, no systematic study has been performed on the potential antitumor ability of nonfunctionalized crown compounds. The fact that some crown ethers showed antiproliferative activity[13] and that some ionophores, such as valinomycin, an antibiotic with potassium-selective ionophoric activity, have been reported to display antitumor effects, together with the recent studies on the potential cytotoxicity caused by disrupted ion transport by Gokel group,[14,15] inspired us to check the possible antiproliferative/antitumor ability of crown ethers. We report the antiproliferative activity and structure−activity relationship of several conventional crown ethers and their derivatives in vitro and compare this activity to that of valinomycin. Also, we have attempted to (i) computationally model the relationship of molecular structure to the biological activity of tested crown ethers, (ii) apply the SAR model to a series of previously published alkyl-substituted lariat ethers,[14] and (iii) evaluate the impact of various molecular descriptors on the IC_{50} values of these compounds. Finally, we give a hint to possible mechanisms of action of these compounds, as well as their potential use in anticancer therapy.

Results and Discussion

Antiproliferative Activity. 1−16 and valinomycin were tested for their potential antiproliferative effects on a panel of five human cell lines derived from five cancer types (Experimental Section). We have chosen various derivatives of the 18-crown-6 compound, as first discovered and most frequently

* Corresponding author. Phone: +385 1 4571 235. Fax: +3851 4561 010. E-mail: mhorvat@irb.hr.
[†] Laboratory of Functional Genomics.
[‡] Laboratory for Information Systems.
[§] Laboratory of Supramolecular and Nucleoside Chemistry.
[||] Laboratory for Chemical Kinetics and Atmospheric Chemistry.

10.1021/jm061162u CCC: $37.00
Published on Web 02/15/2007

studied crown ether compounds (**1**−**6**, **11**, **13**, and **14**), along with one derivative with 15 ring atoms (**10**) and two derivatives with larger macrocyclic rings: dibenzo-24-crown-8 and dibenzo-30-crown-10 (**8** and **9**) (**Table 1**). Also, we tested the cell-growth influence of diphenolic (**7**) and diamino (**12**) intermediates in the synthesis of crown ethers **6** and **11**, respectively, and two starting diol reactantants, *tert*-butylcatechol (**15)** and *N*-benzyl-diethanolamine **(16**), to evaluate any potential differences in activity between parts of the crown ether molecule and the entire molecule. As shown in Table 2 and Figure 1,A−F, the tested compounds showed different antiproliferative effects on the presented panel cell lines. In the 18-crown-6 group, **1** had a weak growth-inhibitory effect, predominantly at the highest tested concentration, whereas all other derivatives with various substituents (dicyclohexano, di-*tert*-butyldicyclohexano, dibenzo, di-*tert*-butyldibenzo, and bis(di-*tert*-butylbenzo)) had much stronger effects in the following order: **4** < **6** ≤ **2** < **5** < **3**. This clearly demonstrates that the substituents are of great importance for this effect and that one *tert*-butyl group attached to either a cyclohexyl or a benzyl group potentiates the activity, with di-*tert*-butyldicyclohexano being much stronger. The substitutents obviously increase the hydrophobicity of these compounds, which was confirmed by calculating the log *P* value (partition coefficient between water and octanol) (Table 1). We assume that this hydrophobic surrounding enables the insertion into the cell's membrane and cation transport, which is in accordance with previously published results on antimicrobial or cytotoxic activity of crown ethers.[14−16] Because the 18-, 24-, and 30-membered crown ether compounds were found to more strongly enhance the membrane permeability of potassium in comparison to sodium and calcium ions,[16,17] it might be presumed that the changes in potassium transport are responsible for this effect. However, it has been previously demonstrated in the literature that the relative efficacies of various crown ether compounds to enhance the ability of major physiological cations to cross artificial phospholipid membranes are dependent on ion-binding constants, pH, ion and ionophore concentrations, and the presence of other ions.[16] Therefore, the mechanism by which crown ethers facilitate ion transport through biological membranes is very complicated, and the binding constants for either potassium, sodium, or other important ions are certainly not the crucial transport parameter. Because ion-binding constants and ion selectivity depend on the solvent as well as the ligand,[18] the ability of macrocycles to specifically effect ion-transport processes in cell membranes varies considerably depending on their molecular environment within the membrane. It may be presumed that the solvent media effects primarily arise from differences in the ion and ligand solvations. A larger solvation effect is expected for the smaller sodium ion with high charge density than is expected for the potassium ion, and consequently, a lower mobility is obtained for the sodium complexes. These findings agree with the assumption that complexes of potassium should be more acceptable to a lipid phase than the sodium species. Such effects can be generalized for natural systems and should significantly account for a greater resistance of sodium against complexation with natural carriers.

Dibenzo-24-crown-8 (**8**) has an effect similar to, but a bit less pronounced than that of dibenzo-18-crown-6 (**4**), which correlates with its slightly lower potassium binding ability. However, dibenzo-30-crown-10 (**9**) has a somewhat stronger effect, possibly because these large and highly flexible macrocycles could completely enclose the potassium cation[19] like the naturally occurring cyclic ionophores valinomycin and nonactin.[20,21] It is worth noting that the 18-crown-6 (**1**) with a planar polyether cavity, optimal for the complexation of the potassium ion, has been found to possess the least effective ionophore for potassium, because axial positions of the crown complex are not well protected from the hydrophobic environment existing in the membrane. This fact enables other interactions of the complex, for example, with anion and solvent. These interactions are much less pronounced in the substituted 18-crown-6-ethers, especially in those with the bulky *tert*-butyl groups (**3** and **5**). The somewhat lower activity of crown ether **6** could be ascribed to a decrease in its complexing ability toward the potassium ion because of the steric hindrance produced by the *tert*-butyl substituents in the ortho position with respect to the polyether ring.[22] In addition, it should be pointed out that there are no differences in activity between the crown ether **5** used as a mixture of 4′,4″(5″)-di-*tert*-butyl-substituted isomers and that obtained for the corresponding 4′,4″-di-*tert*-butyl-substituted crown compound, indicating that the the *tert*-butyl group in either the 4 or 5 position on the benzene ring does not influence the inhibition ability of these compounds, just as it does not change their complexation properties (data not shown).

The greater activity of dicyclohexano crown ethers (**2** and **3**) with respect to their dibenzo analogues (**4** and **5**) could be ascribed to good solubility of the former compounds, both in the aqueous and in the organic medium. The diphenolic linear polyether **7** has an effect very similar to that of its crown ether analogue **6**. Interestingly, *tert*-butycatehol (**15**) has moderate inhibitory activity, which is in accordance with the previously published cytotoxic potential of catechols.[23]

It is well-known that crown ethers bind alkali and alkaline earth metal cations more strongly than their equally large aza or diaza analogues.[6] Consequently, the aza-crown compounds showed less obvious antiproliferative effects: *N*-benzyl-monoaza-15-crown-5 (**10**), which has a cavity size too small for potassium but optimal for sodium complexation, is completely inactive. Lariat ethers (**13** and **14**) are derivates of the 18-membered diaza-crown with moderate affinity toward complexation and transport of sodium and potassium ions through artificial membranes.[24] The reduced binding strength of **13** is the consequence of the resonance of the amide group (amide sidearm macroring linkage) and increased rigidity of macroring, whereas compound **14** may effectively bind metal cations through interactions of the crown ring and side chain; surprisingly, this compound has lower activity than **13**. **11** has an inhibitory effect compared to **4**, whereas the effect of its open analogue **12** is somewhat less pronounced. As expected, *N*-benzyl-diethanolamine (**16**) has no effect at all.

Unsurprisingly, valinomycin (Val) has a very strong inhibitory effect (IC_{50}'s are in the nanomolar range). It is interesting that the SW 620 cells are most sensitive to Val, whereas MCF-7 cells are exceptionally resistant. We also noticed that this cell line is to some extent resistant to most of the tested crown ether compounds. We could assume that this is due to the deletion mutation of the Caspase 3 gene in this cell line, which is believed to play a pivotal role in apoptotic cell death.[25] As was shown previously, apoptosis is the main mechanism of Val activity and at least of some of the crown compounds (as presented in this study).

Cell Cycle Perturbations and Activation of Apoptosis. To shed more light on the mechanism underlying the antiproliferative activity of some of the most active crown compounds, we tested the influence of compounds **3**, **5**, **6**, and **7** as well as valinomycin on the cell cycle of MiaPaCa-2 cells (Figure 2). Open-chain **7** did not induce any significant influence on the cell cycle, whereas its corresponding crown ether **6** induced

Table 1. Compound Names, Structures, and Calculated Partition Coefficients (log *P*)[a]

No.	Compound	Structure	log *P*
1	18-crown-6		-0.39
2	dicyclohexano-18-crown-6	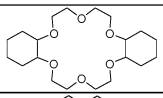	1.45
3	4',4"(5")-di-*tert*-butyldicyclohexano)-18-crown-6, mixed isomers	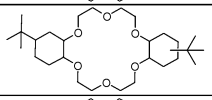	4.63
4	dibenzo-18-crown-6	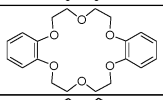	2.35
5	4',4"(5")-di-*tert*-butyldibenzo-18-crown-6, mixed isomers	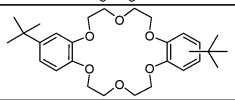	5.40
6	bis(3',5'-di-*tert*-butylbenzo)-18-crown-6	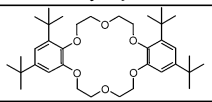	8.08
7	bis[2-(4',6'-di-*tert*-butyl-2'-hydroxyphenoxy)ethyl]ether	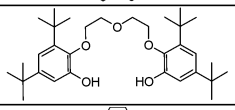	7.81
8	dibenzo-24-crown-8	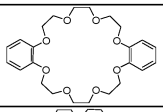	1.85
9	dibenzo-30-crown-10	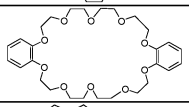	1.52
10	*N*-benzyl-monoaza-15-crown-5	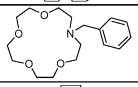	1.13
11	*N*,*N*'-dibenzyl-4,13-diaza-18-crown-6	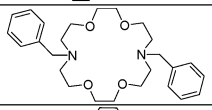	2.35
12	1,10-dibenzyl-4,7-dioxa-1,10-diazadodecan	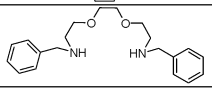	2.21
13	*N*,*N*'-[(*N*''benzyloxycarbonyl) glycyl]-4,13-diaza-18-crown-6	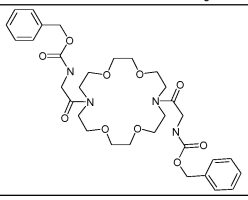	1.54
14	*N*,*N*'-bis(*O*-methyl-D-phenyglycylglycyl)-4,13-diaza-18-crown-6	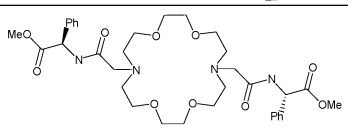	2.27
15	4-*tert*-butylcatechol	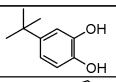	2.78
16	*N*-benzyl-diethanolamine	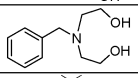	0.70
17	valinomycin	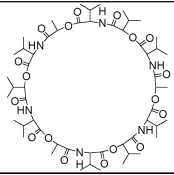	3.18

[a] Octanol−water partition coefficient as computed by ALOGPS 2.1 software.[26]

Table 2. In Vitro Growth Inhibition of Various Tumor-Cell Lines[a]

	IC_{50}[b] (μM)				
compound	H460	HeLa	MiaPaCa−2	SW 620	MCF−7
1	>100	>100	>100	>100	>100
2	16 ± 0.5	25 ± 5	16 ± 3	7 ± 4	36 ± 7
3	0.3 ± 0.04	0.3 ± 0.2	0.3 ± 0.2	0.2 ± 0.05	0.7 ± 0.4
4	28 ± 7	17 ± 8	28 ± 10	17 ± 8	49 ± 22
5	1 ± 0.1	1 ± 0.3	1.8 ± 0.9	1.4 ± 0.02	4.6 ± 2
6	19 ± 8	10 ± 8	15 ± 3	19 ± 0.1	8 ± 9
7	8 ± 5	11 ± 1	18 ± 5	19 ± 1	29 ± 4
8	24 ± 3	21 ± 0.1	32 ± 3	72 ± 29	>100
9	9 ± 3	11 ± 5	7 ± 2	17 ± 1	30 ± 2
10	>100	>100	>100	>100	>100
11	25 ± 7	14 ± 1	23 ± 12	6 ± 5	25 ± 15
12	31 ± 10	24 ± 16	>100	39 ± 20	>100
13	>100	37 ± 4	71 ± 29	40 ± 11	44 ± 2
14	>100	>100	>100	≥100	>100
15	22 ± 4	24 ± 7	20 ± 3	22 ± 6	23 ± 8
16	>100	>100	>100	>100	>100
Val[c]	0.001	0.001	0.001	0.0001	0.5 ± 0.1

[a] The cell growth rate was evaluated after 72 h by MTT assay (Experimental Section). [b] IC_{50} is the concentration that causes 50% growth inhibition. [c] Val stands for valinomycin.

slight G1 arrest and S phase reduction after 48 h of incubation with the compound at IC_{50} concentration (data not shown). However, **5** and **3** induced major cell cycle perturbations at 1 μM, which represents an IC_{50} concentration for **5** and a somewhat higher IC_{50} concentration for **3** ($\sim 5 \times 10^{-7}$ M). The treatment of MiaPaCa-2 cells with **5** and **3** induced continuing accumulation of cells in the G1 phase during 48 h of incubation, with S phase reduction. Moreover, **3** induced a remarkable G1 phase arrest along with a decrease in the number of S phase cells, with an impressive increase in the number of subG1 cells (representing the apoptotic cells) after 48 h. A comparable but more dramatic effect was noticed after the treatment of MiaPaCa-2 cells with valinomycin at 10 nM. Like **3**, only a modest effect was obtained using the IC_{50} concentration ($\sim$1 nM, data not shown). Valinomycin induced a time-dependent accumulation of cells in the G1 phase, a reduction of the number of cells in the S phase, but a dramatic increase in the number of apoptotic cells, even after 24 h of incubation. These results are in good agreement with the published literature, because it is well-known that valinomycin is a potent inducer of apoptosis in many cell types.[27,28] However, there is very little evidence about its effect on the cell cycle changes. For example, Kleuser et al.[29] showed that valinomycin inhibited proliferation of many cell lines with a saturating effect from about 20 to 100 nM and that nontransformed cells were proliferation-arrested by valinomycin essentially in the G1 phase of the cell cycle, whereas not all transformed cells under this condition were arrested selectively in G1. This is partially in accordance with our results, because in our experiments transformed cells were arrested in the G1 phase.

It has been recognized that potassium currents play a role in cell proliferation, specifically in the regulation of progression through the G1 phase, although there are contradictory results and the exact mechanism remains unclear. The strong G1 arrest of cells after treatment with **3** and **5** points to the role of potassium transport in the progression through the G1 phase of the cell cycle. Our results are in accordance with the observation described by Wible et al.[30] who showed that increased K^+ efflux induced an increase in the population of cells in the G1 phase after 24 h, followed by a dramatic increase of apoptotic cells (after 72 h).

Indeed, many published reports suggest that the regulation of K^+ fluxes has a major impact on apoptosis as well as on proliferation regulation, especially in the G1 transition regulation. Most papers support the notion that the K^+ efflux induces apoptosis by disrupting either mitochondrial or plasma membrane potential and cell shrinkage. Other studies claim that K^+ channel blockers inhibit proliferation by arresting the cells in the G1 phase, either without activation of apoptosis or even by its inhibition.[31−34] Although there are more and more publications that propose the importance and potentials of K^+ transport regulation in cancer treatment, the evidence for the role of K^+ transport in apoptosis and inhibition of cancer cell growth is conflicting and requires more attention. For example, in some cells, inhibition of K^+ channels appears to favor apoptosis, whereas in other models, apoptosis is activated by K^+-channel-mediated loss of K^+. These discrepancies may be due to the fact that these studies are mostly concerning the activity/expression of various K^+ channels, which are known to be one of the most ubiquitous and diverse families of plasma membrane ion channels and to have a large variety of essential roles in different cells.[31,35] Fewer studies are focused on K^+ ionophores and their potentials in antitumor treatment, with the exception of valinomycin, which was shown to be too toxic. Our results support the hypothesis that the strong antiproliferative activity of various crown ether compounds tested is the result of their activity as membrane-active potassium ion transporters, which may promote K^+ efflux.

However, targeting the cell membrane and disrupting the main physiological cations' homeostasis undoubtedly should have toxic consequences in normal tissue. Indeed, various studies have been performed, and several papers were published more than 20 years ago showing the toxicity of different cationic ionophores (including crown ethers) in multiple species.[16,36−38] These studies unequivocally showed that the majority of the ionophores induced mainly neurobehavioral toxic effects (tremor, aggressive behavior, muscle contractions), eye and skin irritations, testicular atrophy, and so forth. These effects disappeared after the discontinuance of dosing, supporting the view that the effects seen are of a reversible pharmacological nature.[37,38] Also, it was shown that the lethal concentration (LD_{50}) in mice of several crown ethers was about the same as that found for aspirin.[36] Interestingly, the relative lethality of cyclic polyethers increased with both the ring size and the hydrophilicity, being quite opposite to the onset and extent of neurobehavioral symptoms. Moreover, the attached substituent groups (such as dicyclohexano or dibenzo groups) significantly augment or reduce (respectively) the lethal potency of 18-crown-6 moieties, while having no influence on the neurological signs.[16]

Because no anticancer drug is likely to be free of toxic side effects, we believe that crown ethers (or other membrane-active drugs) should induce toxicities different from those of conventional antitumor drugs and could be used as such. We agree with Marklund et al.[39] that K^+ ionophores could complement existing drugs and provide a valuable adjunct to therapy and should be further evaluated for their potential clinical usefulness. Crown ethers could be among these drugs, because they have a firm foundation in biological science and industry and will produce new and innovative applications with future generations of compounds.[1] This study represents the first experimental attempt to systematically evaluate antitumor potentials of crown ethers. It should form the basis for more detailed studies on either biological mechanisms or novel synthetic approaches focusing on variations of substituent groups that should augment their activity. However, regarding the toxic side effects of membrane-active compounds, new means of providing selectivity between tumor and normal cells should also be considered.

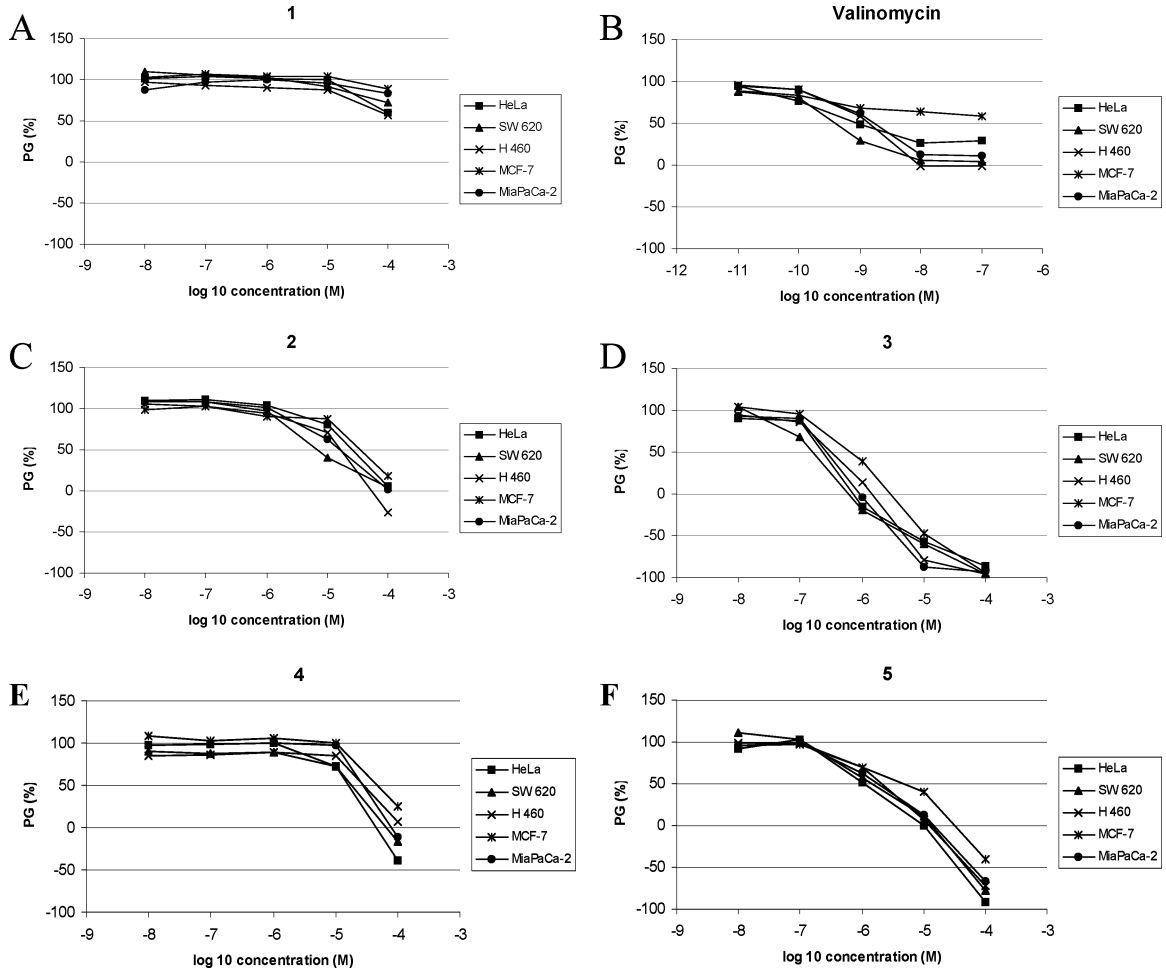

Figure 1. Concentration−response profiles for the representative crown compounds (**1**−**5**) and valinomycin tested on various human tumor-cell lines in vitro. The cells were treated with the compounds at different concentrations, and the percentage of growth (PG) was calculated. Each point represents a mean value of four parallel samples in three individual experiments.

For example, cell targeting can be achieved either by "passive" methods, in which ionophores should be encapsulated or attached to a lipid-based or polymer-based carrier system, or by "active" targeting—the attachment of a homing moiety such as monoclonal antibodies or ligands in the form of peptides, sugars, or lectins—to deliver the potential drug to the right cell by attaching it to specific receptors on cell surfaces.[40] Alternatively, there are several lines of evidence that there are substantial differences between normal and tumor cells with respect to the membrane potentials and potassium and other ion currents and/or concentrations[41−43] that could possibly be exploited for therapy by membrane-active ionophores. Of course, further in vivo studies are needed.

Interactions with Double-Stranded DNA. To exclude the possibility that the crown ether compounds interact with double-stranded DNA and thus exert the antiproliferative (cytotoxic) effect, we tested their potential interactions with calf thymus DNA (ct-DNA) by checking their influence/changes on the thermal stability of ct-DNA (ΔTm). None of the studied compounds influence the thermal stability of ct-DNA within the error of the method (data not shown). Because the studied structures possess neither a condensed aromatic moiety nor any positive charges, the absence of interaction with DNA is not surprising. These results are in accordance with Arenas et al. showing that 18-crown-6 and 21-crown-7 and their dicyclohexyl derivatives are not genotoxic nor do they exhibit co-mutagenic properties.[13]

Computational Modeling of Molecular Structure−Activity Relationship (SAR). Besides the previously described SAR based on domain expert interpretation of molecular properties, we have attempted to computationally model the relationship of molecular structure to biological activity of crown ethers using the support vector machines algorithm for regression (SVM, for details refer to Experimental Section). Chemical descriptor data was transformed using principal component analysis prior to use of SVM to filter out noise and thus reduce the possibility of overfitting (learning complex patterns very specific to training data that have no actual correlation to biological activity). In addition to the use of principal component filtering, crossvalidation methodology is an additional measure against overfitting used in this work. Accuracy of the model on unseen data was assessed by multiple crossvalidation runs, resulting in a Pearson's correlation coefficient of 0.739 between the predicted and actual log IC_{50} values. Such a reasonably high score indicates the model may be of use in predicting the activity of molecules similar in structure and mechanism of action. Conversely, the compounds with the highest crossvalidation error, as shown in Table 3a, may have molecular mechanisms of action different from the rest of the molecules in the training set. **15** (4-*tert*-butylcatechol) is predicted to have much lower activity than was experimentally measured, indicating an alternative mechanism of action. This is completely in accordance with the previously published literature, reporting the cytotoxic potentials of catechols and their corresponding *o*-

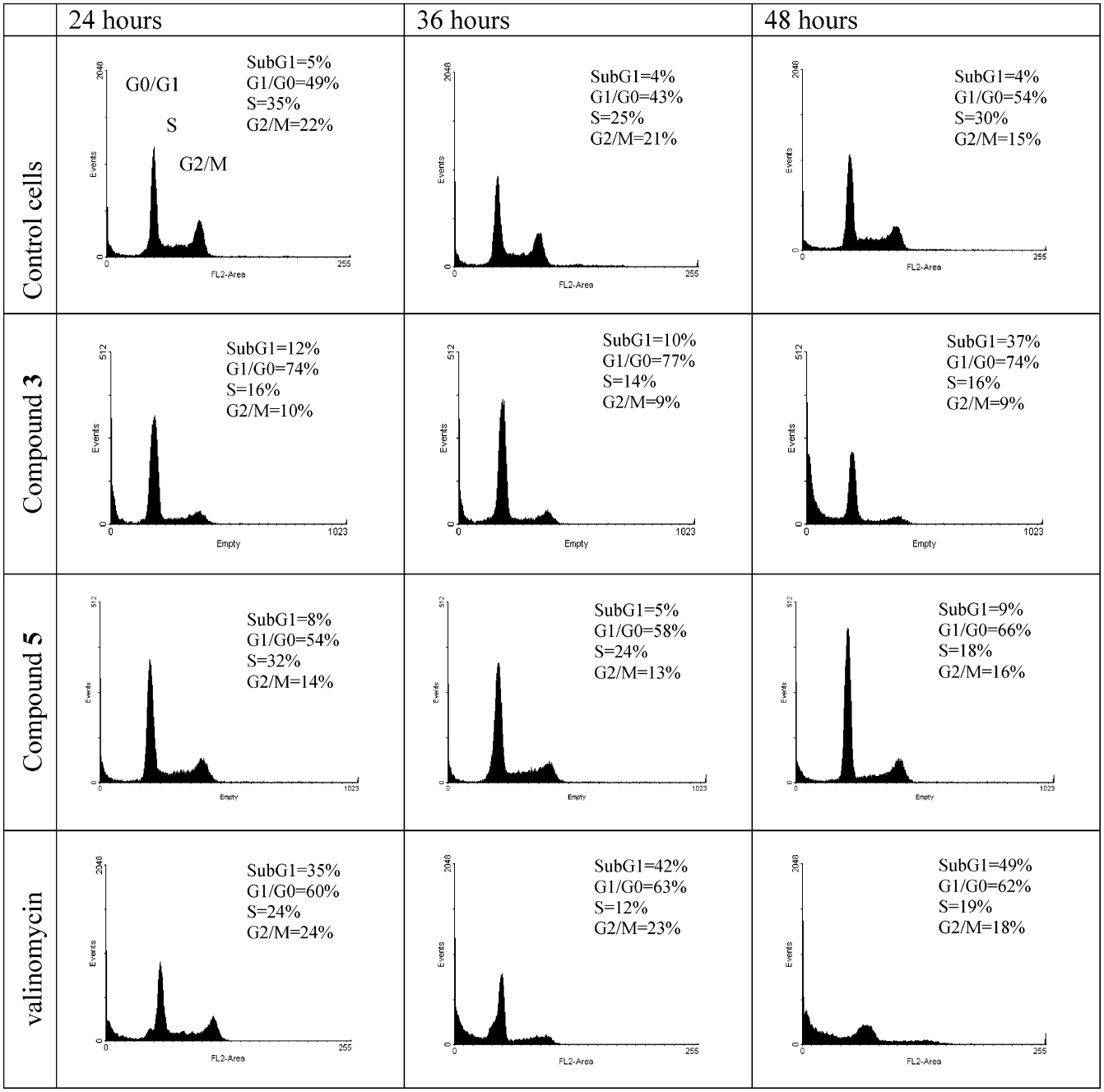

Figure 2. DNA histograms obtained by flow cytometry (Experimental Section), and the percentages of cells in sub G1 (apoptotic cells), G0/G1, S, and G2/M cell cycle phase, after the treatment of MiaPaCa-2 cells with **3** (at 10^{-6} M), **5** (at 10^{-6}M), and valinomicin (10^{-8}M) for 24, 36, and 48 h.

quinones. This activity is attributed to the presence of the catechol group, which is known to undergo one-electron oxidation readily to give the corresponding semiquinone radical. These reactive species may induce cell death mostly through DNA damage (inducing single or double DNA strand breaks), which is contrary to our mechanistic presumptions.[21]

To refine the model, we excluded **15** from the training set and repeated the SVM training procedure; the estimated Pearson's correlation coefficient for unseen data has improved to 0.772. Leave-one-out crossvalidation errors for the molecules in Table 3b hint at possible points of interest in the mechanism of action for **9** and **14**. Dibenzo-30-crown-10 (**9**) has shown better inhibitory activity than predicted; we suspect this might be due to different complexation properties. Namely, as discussed previously, the crystal structures of the complexes also reflect the spatial relations between ligand cavity and cation diameter.[17] With increasing ring width and flexibility, crown ether ligands are inclined to complex with cations that are too small by twining around them; for example, the ligand conformation in the 1:1 complex of **9** with K^+ is similar to the shape of a tennis ball fissure.[6,44] However, **14** is less active in experiment than the model would predict, which might be related to unfavorable distribution of functional groups in the crown side chains that the model does not capture.

Both the starting (16-molecule) and the refined (15-molecule) model had high estimated performances on unseen data when the two strongest principal components (PCs) of the chemical descriptor space were used. Relying on only two very general directions of variation (containing ∼66% of the original descriptor information), the model is not likely to overfit and should be generalizable to a wider set of crown ether-like compounds. The models can also be easily visualized, as

Table 3. Comparison of Measured Average (Over Five Cell Lines) log IC_{50} Values to Predictions Obtained Using Leave-One-Out Crossvalidation on the SVM Regression Model[a]

part a[b]							part b[c]						
	activity (log IC_{50})			rank				activity (log IC_{50})			rank		
cmpd	act	pre	err	act	pre	err	cmpd	act	pred	err	act	pre	err
1	−2.8	−1.93	0.87	14	16	2	**1**	−2.8	−2.911	−0.111	13	14	1
2	−4.75	−4.452	0.298	7	5	2	**2**	−4.75	−4.166	0.584	7	6	1
3	−6.49	−4.963	1.527	1	3	2	**3**	−6.49	−4.183	2.307	1	5	4
4	−4.59	−3.939	0.651	9	9	0	**4**	−4.59	−3.451	1.139	8	10	2
5	−5.76	−5.585	0.175	2	1	1	**5**	−5.76	−4.349	1.411	2	2	0
6	−4.88	−4.18	0.7	4	6	2	**6**	−4.88	−4.313	0.567	4	3	1
7	−4.82	−5.014	−0.194	5	2	3	**7**	−4.82	−4.35	0.47	5	1	4
8	−4.29	−3.981	0.309	11	8	3	**8**	−4.29	−3.955	0.335	10	9	1
9	−4.9	−4.46	0.44	3	4	1	**9**	**−4.9**	**−3.957**	**0.943**	**3**	**8**	**5**
10	−2.5	−3.312	−0.812	15	12	3	**10**	−2.5	−3.253	−0.753	14	12	2
11	−4.79	−4.161	0.629	6	7	1	**11**	−4.79	−4.217	0.573	6	4	2
12	−4.31	−3.851	0.459	10	11	1	**12**	−4.31	−3.391	0.919	9	11	2
13	−4.13	−3.181	0.949	12	13	1	**13**	−4.13	−2.968	1.162	11	13	2
14	−3.03	−3.867	−0.837	13	10	3	**14**	**−3.03**	**−4.012**	**−0.982**	**12**	**7**	**5**
15	**−4.65**	**−3.003**	**1.647**	**8**	**15**	**7**	**15**	n/a	n/a	n/a	n/a	n/a	n/a
16	−2.5	−3.151	−0.651	15	14	1	**16**	−2.5	−2.608	−0.108	14	15	1

[a] Rows in bold are molecules with the highest error in rank. [b] Relates to the first iteration of model building containing 16 molecules in the training set. [c] Relates to the second iteration trained on 15 molecules (4-*tert*-butylcatechol was excluded).

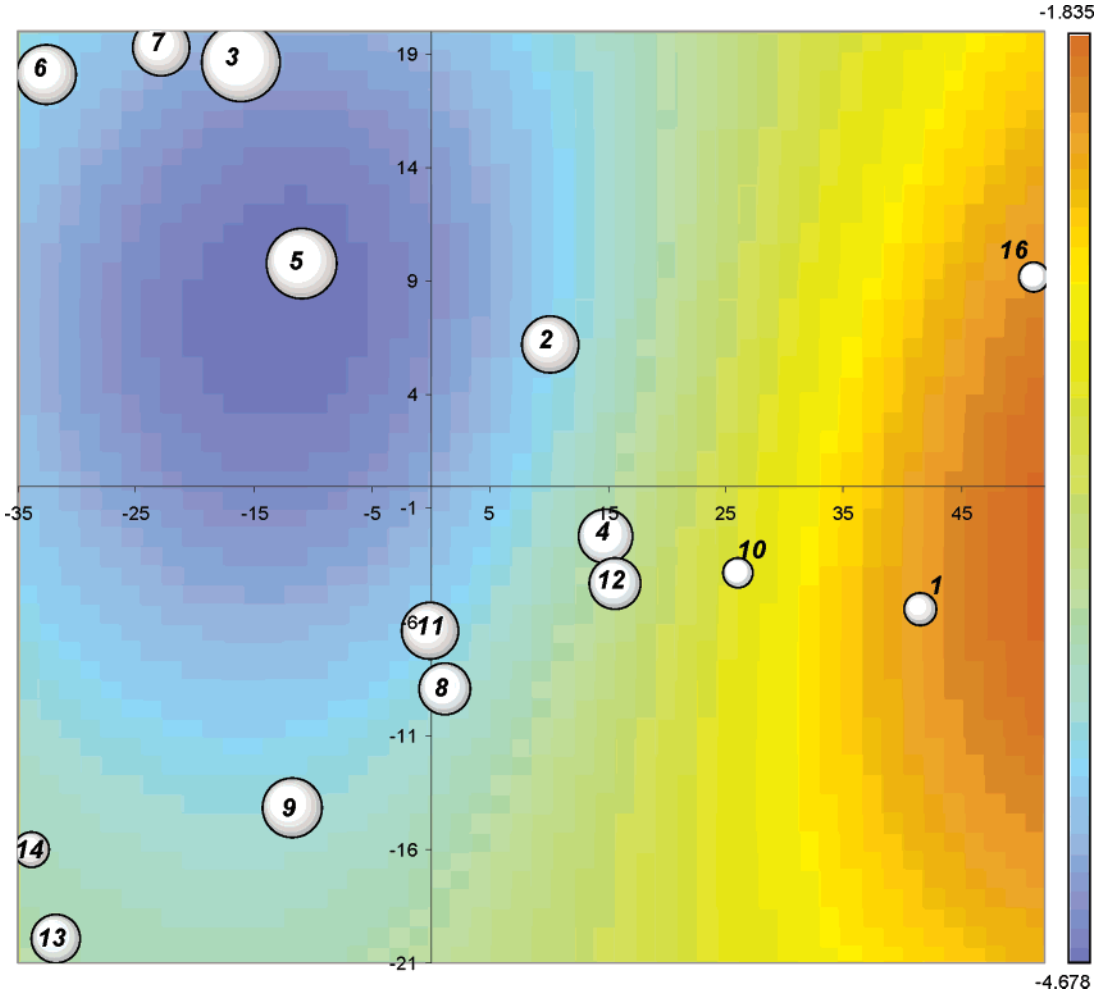

Figure 3. Heatmap visualization of the SVM regression model trained on the refined molecule set (15 molecules, 4-*tert*-butylcatechol excluded). The *x*-axis on the plot corresponds to the first principal component (PC) and the *y*-axis to the second PC. The PCs have no intrinsic interpretation, but they can be explained by correlating them with individual descriptors; the first PC roughly quantifies molecule size and degree of branching, whereas the second PC roughly quantifies molecular shape, symmetry, and hydrophobicity (for details, see text). The background color illustrates the activity (as log IC_{50}), with more active in blue and less active in orange, predicted by the model. The radius of the disk is proportional to the experimentally measured activity (as log IC_{50}) of each compound.

depicted in Figure 3, where the first PC is the *x*-axis and the second PC the *y*-axis. The PCs have no intrinsic interpretation, but they can be explained by correlating them with individual descriptors (data not shown); the first PC in our refined model roughly quantifies molecule size and degree of branching (e.g., constitutional and geometrical descriptors), whereas the second

Table 4. Top 20 Molecular Descriptors Ordered by Average Leave-One-Out Crossvalidation Rank of ReliefF Attribute Ranking Scheme Applied to Refined (15-Molecule) Set[a]

average rank	variation in rank	e-Dragon descriptor	explanation
10.1	± 6.5	BELv2	lowest eigenvalue n. 2 of Burden matrix weighted by atomic van der Waals volumes
10.7	± 8.46	nR06	number of 6-membered rings
12.9	± 10.74	Mor13p	3D-MoRSE - signal 13 weighted by atomic polarizabilities
13.6	± 7.29	BELp2	lowest eigenvalue n. 2 of Burden matrix weighted by atomic polarizabilities
13.8	± 12.82	DISPp	d COMMA2 value weighted by atomic polarizabilities
17.5	± 10.46	BELm2	lowest eigenvalue n. 2 of Burden matrix weighted by atomic masses
19.9	± 9.84	BEHp2	highest eigenvalue n. 2 of Burden matrix weighted by atomic polarizabilities
20.2	± 11.14	BELe2	lowest eigenvalue n. 2 of Burden matrix weighted by atomic Sanderson electronegativities
20.3	± 6.68	ALOGPS_logS	aqueous solubility calculation (ALOGpS)
22.2	± 10.26	BEHv2	highest eigenvalue n. 2 of Burden matrix weighted by atomic van der Waals volumes
22.9	± 16.54	DISPv	d COMMA2 value weighted by atomic van der Waals volumes
23.1	± 27.47	nBM	number of multiple bonds
23.4	± 53.86	nBnz	number of benzene-like rings
23.4	± 54.35	nAB	number of aromatic bonds
23.6	± 54.03	nCar	number of substituted aromatic C(sp2)
26	± 55.31	HOMT	HOMA total
29.8	± 11.18	BEHm2	highest eigenvalue n. 2 of Burden matrix weighted by atomic masses
30.1	± 11.8	BEHe2	highest eigenvalue n. 2 of Burden matrix weighted by atomic Sanderson electronegativities
30.8	± 18.84	Mor13v	3D-MoRSE - signal 13 weighted by atomic van der Waals volumes
41.9	± 34.2	Mor06m	3D-MoRSE - signal 06 weighted by atomic masses

[a] "Variation in rank" represents the maximum deviation of rank, positive or negative, in a single crossvalidation fold from the average over all of the crossvalidation folds.

PC roughly quantifies molecular shape, symmetry, and hydrophobicity (e.g., GETAWAY, topological, and MLOGP, ALOGP, and related descriptors).

Determining Relative Descriptor Relevance. Our first attempt to relate the biological activity of crown ethers to their molecular properties was an examination of log *P* (octanol−water partition coefficient, quantitative descriptor of lipophilicity) values, because we expected that the activity of this group of molecules strongly depends on their ability to remain membrane-bound. The linear regression model predicting log IC_{50} values from the ALOGPS_logP descriptor as computed by e-Dragon[24] ($\log IC_{50} = -0.6685 \cdot \text{ALOGPS\_logP} - 4.3013$) had a leave-one-out crossvalidation correlation coefficient of 0.440 on the refined dataset (no 4-*tert*-butylcatechol), being slightly below the threshold of statistical significance at $p < 0.05$ and faring quite worse than the full SVM model described above. Also, we have attempted to fit a linear model that predicts cytotoxic activity from K^+ binding constants (although they are not molecular descriptors as such), given that we assumed that potassium−crown ether complexation should be an important factor for the membrane transport of potassium ions (data not shown). The use of leave-one-out crossvalidation on the nine compounds with measured K^+ binding constants reveals that not even an approximate linear relationship between the two properties can be established, indicating that some additional molecular properties determine the biological activity of crown ethers, possibly as a result of requirements for membrane insertion. Because of this, it was necessary to use a method that would take into account many descriptors at once, their possible interactions, and one that would allow for nonlinear dependencies.

The ReliefF[45] attribute ranking scheme was used to evaluate the impact of each descriptor computed by the e-Dragon software for the IC_{50} values of the compounds. ReliefF has been shown to be quite robust in situations with many irrelevant attributes and corruption in the target variable;[46] the use of crossvalidation also permits the reliability of ReliefF's predictions to be assessed. Table 4 demonstrates that two main groups of attributes have consistently shown a very high rank and therefore have a high probability of being related to the antiproliferative activity of tested crown ethers, representing versions of the BCUT (e.g., BELv2, BELp2, BELm2, etc.) and d COMMA2 (DISPp and DISPv) descriptors.[47] BCUT descriptors are structure-based molecular descriptors for the representation of low-dimensional chemistry spaces. BCUT spaces are derived from multiple 2D and 3D descriptors by eliminating correlated and statistically insignificant features.[48] BCUT is a class of molecular descriptors defined as eigenvalues of the modified connectivity matrix, which is also called the Burden matrix B. These descriptors have been demonstrated to reflect relevant aspects of molecular structure and are therefore useful in similarity searching and comparison, mostly for molecules known to be active at a particular target. Therefore, BCUT descriptors provide rough indications of how atomic properties relevant to ligand−receptor interaction are distributed.[49] Among BCUT descriptors, BELv2 (the lowest eigenvalue no. 2 of the Burden matrix weighted by atomic van der Waals volumes) has the highest rank. It was shown that the lowest eigenvalues contain contributions from all atoms and thus reflect the topology of the whole molecule.[42] COMMA 2 are geometrical descriptors, where DISPp involves weighting by polarizabilities and DISPv by van der Waals volumes. These descriptors quantify the relative orientation and asymmetry of hydrophobic groups to the general shape of the molecule and distribution of the polarizable (or voluminous in case of DISPv) elements.[40] Taken all together, the 3D structure, the orientation and asymmetry of hydrophobic groups, and the distribution of polarizable elements are of the highest importance for the activity of tested crown ether compounds. This activity is connected to the interaction of the compounds with the receptor/target, which is most likely the membrane. The distributions of polarizable elements influence their ability to complex with metal ions. This is in agreement with previous investigations that crown ethers could only transport metal ions through membranes if both prerequisites for ion complexations (polarizable atoms) and hydrophobicity (membrane penetration) were met. Not surprisingly, calculated aqueous solubility has also shown a very high rank. The solubility of druglike compounds is a very important molecular property that influences the uptake, distribution, transport, and bioavailability of the drugs in the site of action.

Application of Computational Model to Alkyl Derivatives of Diaza-18-crown-6.[14] In the paper by Leevy et al.,[14] the authors have determined minimum inhibitory concentrations of several alkyl-substituted lariat ethers on *E. coli*, *B. subtilis*, and yeast. We could not directly use the data as a test set, because both the test system (mammalian cells vs bacteria and yeast) and the assay used differ between experiments. However, general observations on the results should still hold true. The SVM regression model training procedure, explained in detail in the Experimental Section, was repeated on the 15 molecules with experimentally determined IC_{50} values (4-*tert*-butylcatechol excluded), adding 7 crown ethers with varying side chain lengths (C_8-C_{16}) and functional groups: (C═O)C_9 and (C═O)C_{11} from Leevy et al. were included. The predictions (data not shown) agree with the findings of Leevy et al. with respect to molecules with varying alkyl side chain lengths, where $C_{10} > C_{12} > C_8 > C_{14} \geq C_{16}$. The compounds with 10 and 12 C atoms are most highly active, and the activity drops either with shorter side chains, which are presumably not hydrophobic enough to enter cell membranes, or with side chains that are too long and may interfere with the "flip-flop" ability. Our model could not reproduce the effect of abolishing activity (data not shown) by adding a carbonyl group next to the nitrogen in the macroring, presumably by making the macroring more rigid and/or lessening its affinity for cations. This is not unexpected, because our training set contains only a single molecule (**13**) containing such an amide group. A general qualitative agreement between the two sets of results with regard to varying alkyl side chain lengths indicates the crown ethers examined in this work having a requirement for membrane integration similar to those in Leevy et al., a prerequisite for potassium cation membrane transport.

Conclusions

Although crown ethers have been a topic of great interest in chemical and biological research for more than four decades, no systematic study has been performed on the potential antitumor ability of crown ether compounds. The here-presented study demonstrates the antiproliferative ability and structure−activity relationships of 14 crown and aza-crown ether analogues on five tumor-cell types. The results clearly reveal that crown ethers possess marked tumor-cell growth inhibitory activity and that this activity strongly correlates with both the type of hydrophilic cavity (the size and the nature of donor atoms) and the characteristics of surrounding hydrophobic ring. The most active compounds were di-*tert*-butyldicyclohexano-18-crown-6 (**3**), which exhibited cytotoxicity in the submicromolar range, and di-*tert*-butyldibenzo-18-crown-6 (**5**) (IC_{50} values of $\sim 2\ \mu M$). Also, **3** and **5** induced a marked influence on the cell cycle phase distribution—they induced a strong G1 arrest, followed by the induction of apoptosis. Similar results were obtained using valinomycin. Computational SAR modeling revealed the following: (i) two very general sources of variation in the dataset can be used to model the activity of crown ethers with reasonable confidence, (ii) *tert*-butylcatechol has a mechanism of cytotoxicity different from that of the crown ethers, and (iii) the same structural features are likely important for the activity of the molecules in this work as are important for the molecules in Leevy et al.,[14] implying similar requirements for cell membrane penetration. With regard to impact of individual molecular descriptors on crown ether IC_{50} values, BCUT and d COMMA2 descriptor groups were ranked highly. This points to the importance of the whole molecule topology, orientation, and asymmetry of hydrophobic groups and the distribution of polarizable elements for the interaction with target molecules(s), presumably cell membranes.

Finally, the here-presented results support the hypothesis that crown ether compounds could inhibit tumor-cell growth by disrupting potassium ion homeostasis, which in turn leads to cell cycle perturbations and apoptosis. Further in vitro and in vivo studies with more crown compounds should be performed to support this hypothesis and evaluate their potential clinical usefulness.

Experimental Section

Chemistry. Macrocyclic polyethers 18-crown-6 (**1**), dicyclohexano-18-crown-6 (**2**), 4′,4″(5″)-di-*tert*-butyldicyclohexano-18-crown-6 as mixed isomers (**3**), dibenzo-18-crown-6 (**4**), 4′,4″(5″)-di-*tert*-butyldibenzo-18-crown-6 as mixed isomers (**5**), dibenzo-24-crown-8 (**8**), and dibenzo-30-crown-10 (**9**), as well as 4-*tert*-butylcatechol (**15**) obtained commercially, were purified by repeated recrystallizations from the appropriate solvents: acetonitrile (**1**), *n*-hexane (**2**, **3**, and **9**), acetone (**4**), methanol (**8**), and *n*-heptane (**15**), respectively. Bis(4′-di-*tert*-butylbenzo)-18-crown-6, used for comparison purposes with respect to polyether **5** and bis(3′,5′-di-*tert*-butylbenzo)-18-crown-6 (**6**) were prepared and purified as previously described.[2,50,51] Bis[2-(4′,6′-di-*tert*-butyl-2′-hydroxyphenoxy)ethyl]ether (**7**) was prepared by attaching a base-stable protecting tetrahydropyranyl group to one of the hydroxyls of the di-*tert*-butyl-substituted catechol. Two moles of this compound were then condensed with bis(2-chloroethyl)ether, and the protecting group was subsequently removed by diluted hydrochloric acid. The obtained compound was recrystallized twice from methanol (yield 34%; mp = 196−197 °C; Anal. calcd. for $C_{32}H_{50}O_5$: C, 74.67; H, 9.79%; found: C, 74.85; H, 9.84%). All of the compounds were dried on P_2O_5 in a vacuum at room temperature and stored in a drybox before use.

Aza-crown ethers *N*-benzyl-monoaza-15-crown-5 (**10**)[52] and *N*,*N*′-dibenzyl-4,13-diaza-18-crown-6 (**11**),[53] lariat ethers *N*,*N*′-[(*N*″-benzyloxycarbonyl)glycyl]-4,13-diaza-18-crown-6 (**13**)[22] and *N*,*N*′-bis(*O*-methyl-D-phenylglycylglycyl)-4,13-diaza-18-crown-6 (**14**),[46] and 1,10-dibenzyl-4,7-dioxa-1,10-diazadodecan (**12**)[46] and *N*-benzyl-diethanolamine (**16**)[45] were prepared and purified as previously described.

Antiproliferative Activity. The HeLa (cervical carcinoma), MCF-7 (breast carcinoma), SW 620 (colon carcinoma), MiaPaCa-2 (pancreatic carcinoma), and H460 (lung carcinoma) cells (obtained from American Type Culture Collection ATCC, Rockville, MD) were cultured as monolayers and maintained in Dulbecco's modified Eagle's medium (DMEM) supplemented with 10% fetal bovine serum (FBS), L-glutamine (2 mM), penicillin (100 U/mL), and streptomycin (100 μg/mL) in a humidified atmosphere with 5% CO_2 at 37 °C.

The growth inhibition activity was assessed as described previously, according to the slightly modified procedure of the National Cancer Institute, Developmental Therapeutics Program.[54,55] The cells were inoculated onto standard 96-well microtiter plates on day 0. The cell concentrations were adjusted according to the cell population doubling time (PDT): 1×10^4/mL for HeLa, H460, MiaPaCa-2, and SW 620 cell lines (PDT = 20−24 h) and 2×10^4/mL for MCF-7 cell lines (PDT = 33 h). Test agents were then added in five, 10-fold dilutions (10^{-8} to 10^{-4} mol/L) and incubated for a further 72 h. Working dilutions were freshly prepared on the day of testing. After 72 h of incubation, the cell growth rate was evaluated by performing the MTT assay, which detects dehydrogenase activity in viable cells. The absorbance (OD, optical density) was measured on a microplate reader at 570 nm. The percentage of growth (PG) of the cell lines was calculated according to one or the other of the following two expressions: If (mean OD_{test} − mean OD_{tzero}) ≥ 0, then PG = 100 × (mean OD_{test} − mean OD_{tzero})/(mean OD_{ctrl} − mean OD_{tzero}). If (mean OD_{test} − mean OD_{tzero}) < 0, then PG = 100 × (mean OD_{test} − mean OD_{tzero})/OD_{tzero}, where the mean OD_{tzero} is the average of the optical density measurements before the exposure of the cells to the test compound, the mean OD_{test} is the average of the optical density measurements after the

desired period, and the mean OD_{ctrl} is the average of the optical density measurements after the desired period with no exposure of the cells to the test compound.

Each test was performed in quadruplicate in three individual experiments. The results are expressed as IC_{50}, which is the concentration necessary for 50% inhibition. The IC_{50} values for each compound are calculated from concentration−response curves using linear regression analysis by fitting the test concentrations that give PG values above and below the reference value (i.e., 50%). However, if for a given cell line all of the tested concentrations produce PGs exceeding the respective reference level of effect (e.g., PG value of 50), then the highest tested concentration is assigned as the default value, which is preceded by a ">" sign. Each result is a mean value from three separate experiments.

Cell Cycle Analysis. In a six-well plate, 2×10^5 cells were seeded per well. After 24 h, the tested compounds were added at various concentrations. After the desired length of time, the attached cells were trypsinized, combined with floating cells, washed with phosphate buffer saline (PBS), and fixed with 70% ethanol. Immediately before the analysis, the cells were washed with PBS and stained with propidium iodide (PI, 2.5 μg/mL) with the addition of RNAse A (0.2 μg/μL). The stained cells were then analyzed with a Becton Dickinson FACScalibur flow cytometer (20 000 counts were measured). The percentage of the cells in each cell cycle phase was determined using ModFit LT software (Verity Software House) on the basis of the DNA histograms.

Interactions with Double-Stranded DNA. Calf thymus *ct*-DNA was purchased from Aldrich, dissolved in sodium cacodylate buffer, $I = 0.05$ mol·dm^{-3}, pH = 7, and additionally sonicated and filtered through a 0.45 μm filter, and the final concentration was determined spectroscopically as the concentration of phosphates.[56,57] Thermal melting curves for DNA and its complexes with studied compounds were determined as previously described by following the absorption change at 260 nm as a function of temperature. The Tm values are the midpoints of the transition curves, determined from the maximum of the first derivative and checked graphically by the tangent method. ΔTm values were calculated by subtracting the Tm of the free nucleic acid from Tm of the complex. The error of determined ΔTm values is ±0.5 °C.

Computational Modeling of Molecular Structure−Activity Relationship. Computation of Molecular Descriptors and Data Preprocessing. To build and test a structure−activity relationship model and determine relative importances of molecular features, we employed the following procedure. Chemical structures of the 16 compounds experimentally tested in this work in the SMILES notation were sent to the E-Dragon Web service[24] (http://www.vcclab.org/lab/edragon/) to compute a total of 1666 molecular descriptors per compound. The same procedure was applied to the 8 compounds from Leevy et al.,[14] where compound 6, diaza-18-crown-6 with *n*-octadecyl side chains, had to be excluded as a result of its size exceeding the limit of the free E-Dragon Web version. Finally, the table for regression modeling was produced by coupling a target variable quantifying the average growth inhibitory activity (log IC_{50} value) over 5 cancer cell lines with molecular descriptors of each of the compounds. Measurements exceeding the highest tested concentration (10^{-4} M) were approximated by extrapolation prior to modeling. The data was loaded into the Weka 3.5.2 data mining software[58] where all the further processing steps were performed. Each attribute (descriptor) was standardized to a mean of 0 and standard deviation of 1. Attributes constant over all instances were removed, leaving 1319 attributes for the 16-molecule training set, or 1320 in the case 7 molecules of Leevy et al. were also included.

Structure−Activity Relationship Modeling. We employed a Support Vector Machine (LibSVM[59] implementation in Weka, ϵ-SVR variety, radial basis function kernel) algorithm to train a regression model that predicts IC_{50} values from the molecular descriptors of the experimentally analyzed compounds and used 100 runs of 4-fold crossvalidation in the Weka experimenter to test its predictive strength. A Pearson's correlation coefficient r was computed between the predicted and the actual log IC_{50} values in each testing fold, and the average of 400 such correlation coefficients (4 times 100 runs) is reported as the estimated model performance on unseen data.

Prior to training, we have applied principal component analysis (PCA) to the data to reduce the number of attributes and filter out noise; normalization in Weka's PCA was turned off as the attributes were already standardized. Retaining 95% of the original descriptor information generated 9 principal components, or 10 if the 7 molecules from Leevy et al. were included. Using Weka Experimenter, we simultaneously optimized (i) the SVM parameter c (controls complexity and generalization properties of models), (ii) the SVM parameter γ (controls the shape of the regression hyperplane), and (iii) the number of principal components discarded to maximize the model performance estimate (r, above). Normalization option of the LibSVM in Weka was switched on; all the other parameters were left at default values. Parameters c and γ were varied exponentially, from 10^{-2} to 10^3 (c) and 10^{-3} to 10^2 (γ) in increments of 10^1; after selection of the optimal number of PCs, c and γ, a second iteration of "fine-tuning" of c and γ was used where the two parameters were varied exponentially from $10^{OptimalValue - 1}$ to $10^{OptimalValue + 1}$ in increments of $10^{0.1}$.

For the original 16-molecule dataset, the highest performance was achieved for two principal components (PCs) $r = 0.739$, $c = 10^{1.1}$, and $\gamma = 10^{1.1}$. For the refined 15-molecule dataset, a highest "peak" in performance was observed at five PCs ($r = 0.785$); however, a close second ($r = 0.772$) was observed with only two PCs at $c = 10^{0.2}$ and $\gamma = 10^{0.4}$. We decided in favor of the latter model because a much simpler representation of the descriptor space with a similar performance is less likely to overfit and therefore more desirable. When molecules from Leevy et al.[14] were added (15 + 7 = 22 molecules), optimal performance ($r = 0.802$, crossvalidation on 15 training set molecules) was achieved for three PCs, $c = 10^{0.5}$ and $\gamma = 10^{0.1}$. The trained SVM model was then used to predict IC_{50} values for the 7 compounds from Leevy et al.

The errors in the predicted activity of the individual molecules were measured by computing the absolute difference between the rank of the predicted log IC_{50} among all of the predictions using leave-one-out crossvalidation and the rank of the actual log IC_{50} among all actual activities.

Determining Relative Descriptor Relevance. To determine relative descriptor importance, we have used the ReliefF ranking scheme[39] that takes into consideration possible nonlinearities and descriptor interactions. In brief, ReliefF functions by examining the linear correlation of each descriptor to the target variable in local neighborhoods of size k, where "locality" is defined using the Euclidean distance in the full attribute space. Noisy data may require setting k to a high value, making the procedure less "local" and more similar to computing a simple Pearson's correlation coefficient of descriptors and the target variable over all data, thus sacrificing the ability to handle nonlinear dependencies and attributes significant only in interaction. To determine the optimal value for ReliefF's parameter k, we ran the *kNN* (k nearest neighbors) classifier in Weka on the dataset with different k values and found that the accuracy of regression measured as the Pearson's correlation coefficient in leave-one-out crossvalidation, peaks at $k = 7$. This is a relatively high value, considering that the maximum k is 14 for this regression problem (15 instances in the training set, after the exclusion of 4-*tert*-butylcatechol). ReliefF was run on all of the data in the original attribute space (PCA was not used), with no distance weighting and using leave-one-out crossvalidation to assess the robustness of the ranking.

Handling of Mixed Isomers in 3 and 5. During the measurement of cytotoxic activity, which formed the base for our computational structure−activity relationship modeling effort, **5** was not a mixture of isomers but a single compound (4′,5″-di-*tert*-butyl-substituted dibenzyl crown), and this was the structure used in all further computation. **3**, however, was a mixture of isomers (as drawn in Table 1) when tested for cytotoxic activity on cell lines. We decided not to include both isomers of this highly active compound in the training set, because this might bias the SVMs regression hyperplane and the ReliefF's descriptor ranking too

strongly toward the molecular characteristics pronounced in **3**. In addition, having two very similar compounds would compromise the use of crossvalidation in optimization of the SVM parameters and determination of the errors of single molecules.

All previous data in this paper was derived by using a single isomer, the 4′,4″-di-*tert*-butyl-substituted dicyclohexyl crown. We have repeated the complete computational procedure with the other isomer, and the results did not qualitatively differ. In the first run of modeling using all 16 molecules, the optimal SVM parameters were $c = 10^{0.8}$ and $\gamma = 10^{0.8}$ with two PCs, and 100 runs of 4-fold crossvalidation yielded an average $r = 0.742$. *tert*-Butylcatechol (**15**) was again the molecule with the highest leave-one-out crossvalidation error; with an absolute difference in rank of 7, followed by **10** with an absolute difference in rank of 5. After the exclusion of *tert*-butylcatechol, the best refined model with 2 PCs had $r = 0.766$ at $c = 10^{0.2}$ and $\gamma = 10^{0.5}$. The best-refined model with 7 molecules from Leevy et al. included as the test set had $r = 0.781$ at $c = 10^{0.6}$ and $\gamma = 10^{0.1}$. A similar ordering by activity of aza-crown molecules with varying alkyl side chain lengths (data not shown) was observed ($C_{10} > C_{12} \approx C_8 > C_{14} \geq C_{16}$), except that C_{12} and C_8 molecules could not be distinguished by predicted activity. Abolished activity due to a carbonyl group added next to the crown was again not captured by the SVM regression model. Among the top 20 descriptors chosen by ReliefF using the 15 molecules containing the 4′,4″-di-*tert*-butyl-substituted dicyclohexyl crown isomer, 17 were also present in the top 20 when the 4′,5″-di-*tert*-butyl isomer was used. "Mor13p", "Mor13v", and "Mor06m" were replaced by "Mor25v", "J3D", and "DISPe". The Spearman rank correlation coefficient among the 17 descriptors present in the both top 20 sets was 0.963, indicating that the ordering of attribute importance was strongly preserved.

Acknowledgment. We thank the Ministry of Science, Education and Sport of Croatia for financial support. We are very grateful to Dr. Sanja Tomić and Dr. Bono Lučić for useful discussions on molecular descriptors.

References

(1) Gokel, G. W.; Leevy, W. M.; Weber, M. E. Crown Ethers: Sensors for Ions and Molecular Scaffolds for Materials and Biological Models. *Chem. Rev.* **2004**, *104*, 2723−2750.
(2) Pedersen, C. J. Cyclic Polyethers and Their Complexes with Metal Salts. *J. Am. Chem. Soc.* **1967**, *89*, 7017−7036.
(3) Lehn, J. M. Supramolecular Chemistry − Scope and Perspectives Molecules - Supermolecules -Molecular Devices. *Angew. Chem., Int. Ed. Engl.* **1988**, *27*, 89−112.
(4) Lehn, J. M. *Supramolecular Chemistry: Concept and Perspectives*; VCH Publishers: Weinheim, 1995.
(5) Cram, D. J. The Design of Molecular Hosts, Guests, and Their Complexes. *Angew. Chem., Int. Ed. Engl.* **1988**, *27*, 1009−1020.
(6) Vögtle, F., Ed. *Host Guest Complex Chemistry I*; Topics in Current Chemistry 98; Springer-Verlag: New York, 1981.
(7) Tso, W.-W.; Fung, W.-P.; Tso, M.-Y-.W. Variability of Crown Ethers Toxicity. *J. Inorg. Biochem.* **1981**, *14*, 237−244.
(8) Arenas, P.; Bitticks, L.; Pannell, K.; Garcia, S. Genotoxic Potential of Crown Ethers in Salmonella Typhimrium. *Mutagenesis* **1989**, *4*, 437−438.
(9) McPhee, M. M.; Kern, J. T.; Hoster, B. C.; Kerwin, S. M. Propargylic Sulfone-armed Lariat Crown Ethers: Alkali Metal Ion-regulated DNA Cleavage Agents. *Bioorg. Chem.* **2000**, *8*, 98−118.
(10) Huang, S.-T.; Kuo, H.-S.; Hsiao, C.-L.; Lin, Y.-L. Efficient Synthesis of Redox-switched Naphtoquinone Thiol-Crown Ethers and their Biological Activity Evaluation. *Bioorg. Med. Chem.* **2002**, *10*, 1947−1952.
(11) Jansen, B. A. J.; Wielaard, P.; den Dulk, H.; Brouwer, J.; Reedijk, J. Oxa-aza Crown Ethers as Ligands for Mixed-Ligand Cisplatin Derivatives and Dinuclear Platinum Anticancer Drugs. *Eur. J. Inorg. Chem.* **2002**, 2375−2379.
(12) McPhee, M. M.; Kerwin, S. M. Synthesis, DNA Cleavage, and Cytotoxicity of a Series of Bis(propargylic)sulfone Crown Ethers. *Bioorg. Med. Chem.* **2001**, *9*, 2809−2818.
(13) Cai, M.-Y.; Arenaz, P. Antimutagenic Effect of Crown Ethers on Heavy Metal-Induced Sister Chromatid Exchanges. *Mutagenesis* **1998**, *13*, 27−32.
(14) Leevy, W. M.; Weber, M. E.; Gokel, M. R.; Hughes-Strange, G. B.; Daranciang, D. D.; Ferdani, R.; Gokel, G. W. Correlation of Bilayer Memebrane Cation Transport and Biological Activity in Alkyl-Substituted Lariat Ethers. *Org. Biomol. Chem.* **2005**, *3*, 1647−1652.
(15) Leevy, W. M.; Gammon, S. T.; Levchenko, T.; Daranciang, D. D.; Murillo, O.; Torchilin, V.; Piwnica-Worms, D.; Huettner, J. E.; Gokel, G. W. Structure-activity Relationships, Kinetics, Selectivity and Mechanistic Studies of Synthetic Hydrophile Channels in Bacterial and Mammalian Cells. *Org. Biomol. Chem.* **2005**, *3*, 3544−3550.
(16) Gad, S. C.; Reilly, C.; Siino, K.; Gavigan, F. A.; Witz, G. Thirteen Cationic Ionophores: Their Acute Toxicity, Neurobehavioral and Membrane Effects. *Drug Chem. Toxicol.* **1985**, 8, 451−468.
(17) Naumowicz, M.; Petelska, A. D., Figaszewski, Z. A. The Effect of the Presence of Crown Ether on Ion Transport Across the Lipid Bilayer. *Cell. Mol. Biol. Lett.* **2003**, *8*, 383 − 389.
(18) Izatt, R. M.; Pawlak, K.; Bradshaw, J. S. Thermodynamic and Kinetic Data for Macrocycle Interaction with Cations and Anions. *Chem. Rev.* **1991**, *91*, 1721−2085.
(19) Matijašić, I.; Dapporto, P.; Rossi, P.; Tušek-Božić, Lj. Conformational Studies of Dibenzo-30-crown-10 Complexes. Synthesis and Crystal Structures of Potassium and Ammonium Hexafluorophosphate Complexes. *Supramol. Chem.* **2000**, *13*, 193−206.
(20) Neupert-Laves, K.; Dobler, M. The Crystal Structure of a K^+ Complex of Valinomycin. *Helv. Chim. Acta* **1975**, *58*, 432−442.
(21) Kilbourn, B. T.; Dunitz, J. D.; Pioda, L. A.; Simon, W. Structure of the K^+ Complex With Nonactin, a Macrotetrolide Antibiotic Possessing Highly Specific K^+ Transport Properties. *J. Mol. Biol.* **1967**, *30*, 559−563.
(22) Tušek-Božić, Lj.; Danesi, P. R. Complexation of Some Substituted Macrocyclic Polyethers with Alkali Metal Cations in Methanol, Dimethylsulfoxide and Acetonitrile. *J. Inorg. Nucl. Chem.* **1979**, *41*, 833−837.
(23) Lam, L. K.; Gark, P. K.; Swanson, S. M.; Pezzuto, J. M. Evaluation of the Cytotoxic Potential of Catechols and Quinones Structurally Related to Butylated Hydroxyanisole. *J. Pharm. Sci.* **1988**, *77*, 393−395.
(24) Žinić, M.; Frkanec, L.; Škarić, V.; Trafton, J.; Gokel, G. W., Dipeptide-Derived Lariat Ethers as Enantioselective Carriers of Z-amino Acid and Dipeptide Carboxylates. *Supramol. Chem.* **1992**, *1*, 47−58.
(25) Yang, X.-H.; Sladek, T. L.; Liu, X.; Butler, B. R.; Froelich, C. J.; Thor, A. D. Reconstitution of Caspase 3 Sensitizes MCF-7 Breast Cancer Cells to Doxorubicin- and Etoposide-Induced Apoptosis. *Cancer Res.* **2001**, *61*, 348−354.
(26) Tetko, I. V.; Gasteiger, J.; Todeschini, R.; Mauri, A.; Livingstone, D.; Ertl, P.; Palyulin, V. A.; Radchenko, E. V.; Zefirov, N. S.; Makarenko, A. S.; Tanchuk, V. Y.; Prokopenko, V. V. Virtual Computational Chemistry Laboratory - Design and Description, *J. Comput.-Aided Mol. Des.* **2005**, *19*, 453−463.
(27) Dallaporta, B.; Marchetti, P.; De Pablo, M. A.; Maisse, C.; Duc, H.-T.; Metivier, D.; Zamzami, N.; Maurice, G.; Kroemer, G. Plasma Membrane Poteintial in Thymocite Apoptosis. *J. Immunol.* **1999**, *162*, 6534−6542.
(28) Yu, S. P.; Yeh, C.-H.; Sensi, S. L.; Gwang, B. J.; Canzoniero, L. M. T.; Farhangrazi, Z. S.; Ying, H. S.; Tian, M.; Dugan, L. L.; Choi, D. W. Mediation of Neuronal Apoptosis by Enhancement of Outward Potassium Current. *Science* **1997**, *278*, 114−117.
(29) Kleuser, B.; Rieter, H.; Adam, G. Selective Effects by Valinomycin on Cytotoxicity and Cell Cycle Arrest of Transformed Versus Nontransformed Rodent Fibroblasts In Vitro. *Cancer Res.* **1985**, *45*, 3022−3028.
(30) Wible, B. A.; Wang, L.; Kuryshev, Y. A.; Basu, A.; Haldar, S.; Brown, A. M. Increased K^+ Efflux and Apoptosis Induced by the Potassium Channel Modulatory Protein KChAP/PIAS3β in Prostate Cancer Cells. *J. Biol. Chem.* **2002**, *277*, 17852−17862.
(31) Lang, F.; Ritter, M.; Gamper, N.; Huber, S.; Fillon, S.; Tanneur, V.; Lepple-Wienhues, A.; Szabo, I.; Gubins, E. Cell Volume in the Regulation of Cell Proliferation and Apoptotic Cell Death. *Cell Physiol. Biochem.* **2000**, *10*, 417−428.
(32) Prado, L. A. Voltage-gated Potassium Channels in Cell Proliferation. *Physiology* **2004**, *19*, 285−292.
(33) Wonderlin, W. F.; Strobl, J. S. Potassium Channels, Proliferation and G1 Progression. *J. Membr. Biol.* **1996**, *154*, 91−107.
(34) Renaudo, A.; Watry, V.; Chassot, A.-A.; Ponzio, G.; Ehrenfeld, J.; Soriani, O. Inhibition of Tumor Cell Proliferation by σ Ligands is Associated With K^+ Channel Inhibition and $p27^{kip1}$ Accumulation. *J. Pharmacol. Exp. Ther.* **2004**, *311*, 1105−1114.
(35) Shieg, C.-C.; Coghlan, M.; Sulivan, J. P.; Gopalakrishnan, M. Potassium Channels: Molecular Defects, Diseases, and Therapeutic Opportunities. *Pharmacol Rev.* **2000**, *52*, 557−593.

(36) Hendrixon, R. R.; Mack, M. P.; Palmer, R. A.; Ottolenghi, A.; Ghirardelli, R. G. Oral Toxicity of the Cyclic Polyethers − 12-Crown-4, 15-Crown-5 and 18-Crown-6 − in Mice. *Toxicol. Appl. Pharmacol.* **1985**, 8, 451−468.
(37) Takayama, K.; Hasegawa, S.; Sasagawa, S.; Nambu, N.; Nagai, T. Apparent Oral Toxicity of 18-Crown-6 in Dogs. *Chem. Pharm. Bull.* 1977, 25, 3125.
(38) Gad, S. C.; Conroy, W. J.; McKelvey, J. A.; Turney, K. A. Behavioral and Neuropharmacological Toxicology of the Macrocyclic Ether 18-Crown-6. *Drug Chem. Toxicol.* 1978, 1, 339−353.
(39) Marklund, L.; Henriksson, R.; Grankvist, K. Cisplatin-induced Apoptosis of Mesothelioma Cells is Affected by Potassium Ion Flux Modulator Amphotericin B and Bumetanide. *Int. J. Cancer* **2001**, *93*, 577−583.
(40) Kralj, M; Pavelic, K. Medicine on a Small Scale. How Molecular Medicine Can Benefit from Self-Assembled and Nanostructured Materials. *EMBO Rep.* **2003**, *4*, 1008−1012.
(41) Killion J. J. Electrical Properties of Normal and Transformed Mammalian Cells. *Biophys J.* **1984**, *45*, 523−528.
(42) Fieber, L. A. Ionic Currents in Normal and Neurofibromatosis Type 1-Affected Human Schwann Cells: Induction of Tumor Cell K Current in Normal Schwann Cells by Cyclic AMP. *J. Neurosci. Res.* **1998**, *54*, 495−506.
(43) Binggeli, R., Cameron, I. L. Cellular Potentials of Normal and Cancerous Fibroblasts and Hepatocytes. *Cancer Res.* **1980**, *40*, 1830−1835.
(44) Vögtle, F., Ed. *Host Guest Complex Chemistry II*; Topics in Current Chemistry 101; Springer-Verlag: New York, 1982.
(45) Kononenko, I. In *Estimation Attributes: Analysis and Extensions of RELIEF*, European Conference on Machine Learning, Catana, Italy, Springer-Verlag, 1994.
(46) Robnik-Šikonja, M.; Kononenko, I. Theoretical and Empirical Analysis of ReliefF and RReliefF. *Machine Learning* **2003**, *53*, 23.
(47) Silverman, B. D. Three-dimensional Moments of Molecular Property Fields. *J. Chem. Inf. Comput. Sci.* **2000**, *40*, 1470−1476.
(48) Xue, L.; Bajorath, J. Molecular Descriptors in Chemoinformatics, Computational Combinatorial Chemistry and Virtual Screening. *Comb. Chem. High Throughput Screening* **2000**, *3*, 363−372.
(49) Todeschini, R.; Consonni, V. In *Handbook of Molecular Descriptors, 11th Ed.*; Mannhold, R., Kubinyi, H., Timmerman, H., Eds.; Wiley-VCH: Weinheim, Germany, 2000.
(50) Tušek, Lj. Two New Alkyl Substituted Aromatic Macrocyclic Polyethers. *Com. Naz. Energ. Nucl., Rapp. Tec.* **1974**, 1−17.
(51) Tušek-Božić, Lj. Conductance Study of Ion-Pairing of Alkali Tetrafluoroborates and Hexafluorophosphates in Acetonitrile Containing Some Substituted Macrocyclic Polyethers. *Electrochim. Acta* **1987**, *32*, 1579−1584.
(52) Schultz, R. A.; White, B. D.; Dishong, D. M.; Arnold K. A.; Gokel, G. W. 12-, 15-, and 18-Membered-Ring Nitrogen-Pivot Lariat Ethers: Syntheses, Properties, and Sodium and Ammonium Cation Binding Properties. *J. Am. Chem. Soc.* **1985**, *107*, 6659−6668.
(53) Gato, V. J.; Arnold, K. A.; Viscariello, A. M.; Miller, S. R.; Morgan C. R.; Gokel, G. W. Syntheses and Binding Properties of Bibrachial Lariat Ethers (BiBLEs): Survey of Synthetic Methods and Cation Selectivities. *J. Org. Chem.* **1986**, *51*, 5373−5384.
(54) Boyd, M. R.; Kenneth, D. P. Some Practical Considerations and Applications of the National Cancer Institute In Vitro Anticancer Drug Discovery Screen. *Drug. Dev. Res.* **1995**, *34*, 91−109.
(55) Malojčić, G.; Piantanida, I.; Marinić, M.; Žinić, M.; Marjanović, M.; Kralj, M.; Pavelić, K.; Schneider, H.-J. A Novel Bis-phenanthridine Triamine with pH Controlled Binding to Nucleotides and Nucleic Acids. *Org. Biomol. Chem.* **2005**, *3*, 4373−4381.
(56) Chaires, J. B.; Dattagupta, N.; Crothers, D. M. Studies on Interaction of Anthracycline Antibiotics and Deoxyribonucleic Acid: Equilibrium Binding Studies on the Interaction of Daunomycin with Deoxyribonucleic acid. *Biochemistry* **1982**, *21*, 3933−3940.
(57) Palm, B. S.; Piantanida, I.; Žinić, M.; Schneider, H.-J. J. The Interaction of New 4,9-Diazapyrenium Compounds with Double Stranded Nucleic Acids *J. Chem. Soc., Perkin Trans.* **2000**, *2*, 385−392.
(58) Witten, I. H.; Frank, E. *Data Mining: Practical Machine Learning Tools and Techniques*; Morgan Kaufmann: San Francisco, 2005.
(59) Chang, C.-C.; Lin, C.-J. *LIBSVM: A Library for Support Vector Machines*, 2001. Software available at http://www.csie.ntu.edu.tw/~cjlin/libsvm.

JM061162U